

TEMPORAL CONTEXT AND ARCHITECTURE: A BENCHMARK FOR NATURALISTIC EEG DECODING

Mehmet Ergezer

School of Computing & Data Science, Wentworth Institute of Technology
Boston, MA USA
Email: ergezerm@wit.edu

ABSTRACT

We study how model architecture and temporal context interact in naturalistic EEG decoding. Using the HBN movie-watching dataset, we benchmark five architectures, CNN, LSTM, a stabilized Transformer (EEGXF), S4, and S5, on a 4-class task across segment lengths from 8 s to 128 s. Accuracy improves with longer context: at 64 s, S5 reaches $98.7\% \pm 0.6$ and CNN $98.3\% \pm 0.3$, while S5 uses $\sim 20 \times$ fewer parameters than CNN. To probe real-world robustness, we evaluate zero-shot cross-frequency shifts, cross-task OOD inputs, and leave-one-subject-out generalization. S5 achieves stronger cross-subject accuracy but makes over-confident errors on OOD tasks; EEGXF is more conservative and stable under frequency shifts, though less calibrated in-distribution. These results reveal a practical efficiency-robustness trade-off: S5 for parameter-efficient peak accuracy; EEGXF when robustness and conservative uncertainty are critical.

Index Terms— EEG decoding, State-space models (S4/S5), Transformers, Naturalistic stimuli, Robustness

1. INTRODUCTION

Decoding brain activity from EEG during naturalistic tasks like movie-watching is a challenging problem, requiring models that capture long-range temporal dependencies from noisy, continuous recordings [1]. While deep learning has been widely applied to EEG, traditional architectures face fundamental trade-offs. CNNs are efficient but constrained by local receptive fields [2,3], while Transformers offer global context via attention [4] but suffer from quadratic scaling in time and memory.

To address these limitations, Structured State-Space Models (SSMs) like S4 [5] and S5/Mamba [6] have emerged, offering a compelling balance of long-range modeling and near-linear computational complexity. Recent studies have applied SSMs to EEG foundation models [7], drowsiness detection [8], and clinical tasks [9, 10]. However, a systematic comparison of how these modern architectures perform against varying temporal context lengths has been missing.

In this work, we investigate the interplay between model architecture and temporal context. We hypothesize that sequence models like S5 and Transformers benefit more from longer EEG segments than local models like CNNs. To test this, we benchmark five architectures on a 4-class naturalistic decoding task using HBN data across segments from 8 s to 128 s. While hybrid architectures like EEG-Conformer [11] achieve state-of-the-art performance by layering mechanisms, we focus on *fundamental* architectural classes (CNN, RNN, SSM, Transformer) to isolate the impact of specific inductive biases. To move beyond simple accuracy, we introduce a suite of challenging generalization tests across unseen tasks, frequencies, and subjects. This evaluation characterizes a fundamental trade-off: S5 offers high speed and accuracy but is prone to overconfidence on out-of-distribution data, whereas EEGXF provides greater robustness.

2. DATASET AND PREPROCESSING

We utilize EEG data from the Healthy Brain Network (HBN) initiative [1], specifically recordings from the movie-watching tasks (“Despicable Me,” “Diary of a Wimpy Kid,” “The Present”) and a resting-state baseline. The raw EEG data was downsampled to 250 Hz, and the first 64 channels were selected. Our preprocessing pipeline consisted of:

1. **Filtering:** Signals were band-passed (1-50Hz). For down-sampling experiments, an anti-aliasing low-pass filter (cut-off $0.45 \times$ target rate) was applied before resampling.
2. **Re-referencing:** Common average reference.
3. **Split & Segmentation:** To prevent data leakage, continuous recordings were **first split** into training (60%), validation (20%), and test (20%) sets. Only then were signals segmented into T -second windows with 50% overlap. This ensures no overlapping windows span across train-test splits.
4. **Normalization:** Each segment was standardized on a per-channel basis (zero mean, unit variance).

Our benchmark uses data from 40 subjects, yielding over 15,000 EEG segments for the 4-class classification task.

3. MODEL ARCHITECTURES

We benchmark five distinct architectures to evaluate the impact of inductive bias: a temporal CNN, a bidirectional LSTM, a vanilla Transformer, our stabilized EEGXF, and the structured state-space model S5. All models accept input tensors of shape (batch, 64, T), where T varies with segment length (e.g., $T = 2000$ for 8 s).

3.1. Structured State-Space Model (S5)

Our S5 classifier builds on recent advances in state-space modeling. It is governed by the continuous-time linear system:

$$\mathbf{h}'(t) = \mathbf{A}\mathbf{h}(t) + \mathbf{B}\mathbf{u}(t) \quad (1)$$

$$\mathbf{y}(t) = \mathbf{C}\mathbf{h}(t) + \mathbf{D}\mathbf{u}(t) \quad (2)$$

In contrast to S4, which uses FFT-based convolutions, S5 directly diagonalizes the state matrix \mathbf{A} to enable an efficient parallel scan. Our implementation uses a stack of 3 bidirectional S5 blocks (hidden dim=192), global average pooling, and a linear classifier. This configuration (183K parameters) allows us to test the efficiency of pure sequence modeling without the quadratic cost of attention.

3.2. EEGXF: A Stabilized Transformer Baseline

Standard Transformers often suffer from training instability on noisy EEG data. To create a robust baseline, we developed EEGXF, a stabilized EEG transformer. Key modifications include a simplified input projection with ReLU activation, multiple BatchNorm layers for stabilization, a conservative encoder with `norm_first=True`, and high-variance weight initialization. Based on hyperparameter sweeps, we utilized a compact configuration (2 layers, 4 heads, $d = 128$, $\text{dropout}=0.1$) which outperformed larger variants. To aggregate temporal features, EEGXF replaces global pooling with a learned attention pooling mechanism.

The CNN (3 layers, 1D convolution) and LSTM (2 layers, bidirectional) serve as standard local and recurrent baselines, respectively. We release all code for reproducibility.¹

4. EXPERIMENTS

Models were trained for up to 100 epochs using the AdamW optimizer, a ‘ReduceLROnPlateau’ scheduler, and early stopping. We used gradient clipping and EMA to stabilize training. Results for 32 s, 64 s, and 128 s are reported as mean \pm std over 3 seeds (CNN/EEGXF/S5); 8s and 16s are single-seed due to cost. Reported training times are wall-clock to early-stopped convergence on a single NVIDIA

¹Code available at: <https://github.com/memoatwit/eeg-s5-benchmark/>

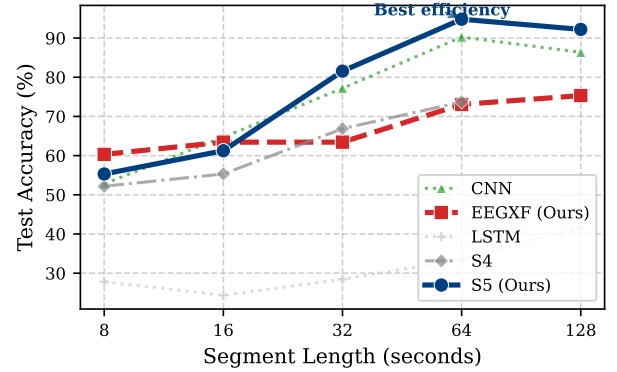


Fig. 1. Test accuracy versus segment length (8–128 s). Single-seed comparison of five architectures (CNN, EEGXF, LSTM, S4, S5). S5 and CNN demonstrate the strongest performance scaling with temporal context; x-axis log-scaled.

RTX 3090 Ti. Unless otherwise noted, Figures 1-2 show single-seed results for five architectures (CNN, EEGXF, LSTM, S4, S5), whereas Table 1 reports mean \pm std over three seeds for our focal models (CNN, EEGXF, S5) at 32/64/128 s to conserve space.

5. RESULTS

Our primary results on subject-mixed splits are summarized in Figure 1 and Table 1². Accuracy improves with longer context: at 64 s, S5 reaches 98.7% \pm 0.6 and CNN 98.3% \pm 0.3, while S5 uses $\sim 20 \times$ fewer parameters than CNN. CNN remains the fastest wall-clock at 64 s (9.8 \pm 0.03 min), and S5 and EEGXF have comparable training times (25.8 \pm 6.2 vs. 25.1 \pm 0.1 min).

The traditional LSTM and our simplified S4 baselines were not competitive. The LSTM failed to converge, and the S4 model, while reaching 73.7% accuracy at 64 s, was prohibitively slow; details in Fig. 2. Figure 2 further illustrates the accuracy-efficiency trade-offs, showing S5 and CNN as the most efficient high-performing architectures.

To further analyze classification behavior, we examined the confusion patterns between the three movie classes at the 64 s segment length (Table 2). Both S5 and CNN demonstrate high precision, misclassifying only 2.7% of movie segments. In contrast, EEGXF exhibits significant confusion between movies (32.4%), explaining its lower F1-score and highlighting its difficulty in separating the nuanced features of the different naturalistic stimuli compared to S5 and CNN.

Figure 2 displays the performance vs efficiency across architectures. S5 models occupy the top-left region of the efficiency-accuracy space, showing they achieve strong per-

²Subject-mixed: train/test split includes overlapping subjects. Subject-independent results are detailed in Sections 5.2, 5.3.

Table 1. Performance on 4-class subject-mixed EEG classification. 32/64/128 s are mean \pm std over 3 seeds; 8/16s are single-seed.

Model	Seg (s)	Acc. (%)	F1	Time (min)
S5 (SSM)	8	55.3	0.55	3.9
	16	61.3	0.61	5.1
	32	94.4 \pm 0.7	0.93 \pm 0.013	19.9 \pm 2.2
	64	98.7 \pm 0.6	0.98 \pm 0.011	25.8 \pm 6.2
	128	95.8 \pm 0.6	0.93 \pm 0.007	17.8 \pm 4.8
EEGXF (Transformer)	8	60.3	0.61	16.2
	16	63.4	0.64	22.9
	32	80.1 \pm 2.0	0.75 \pm 0.029	35.8 \pm 0.3
	64	81.8 \pm 1.8	0.73 \pm 0.019	25.1 \pm 0.1
	128	76.7 \pm 1.5	0.53 \pm 0.032	6.3 \pm 2.6
CNN (Local)	8	52.8	0.53	0.9
	16	64.7	0.65	1.2
	32	94.5 \pm 0.3	0.93 \pm 0.004	7.5 \pm 0.02
	64	98.3 \pm 0.3	0.98 \pm 0.004	9.8 \pm 0.03
	128	89.2 \pm 1.5	0.68 \pm 0.097	6.4 \pm 0.06

Table 2. Inter-movie confusion analysis at 64 s segments. The metric shows the percentage of movie segments incorrectly classified as a different movie.

Model	Movie Confusion Rate (%) \downarrow
S5	2.7%
CNN	2.7%
EEGXF	32.4%

formance with minimal resources. In contrast, EEGXF models trade robustness for compute cost.

5.1. Cross-Frequency Robustness

To assess generalization across EEG sampling rates, we conducted a zero-shot evaluation on subject-independent splits. Models were trained at 250Hz and tested on signals down-sampled to 128Hz and 64Hz using FIR filtering. The results are shown in Table 3 and Figure 3. S5’s accuracy drops significantly (over 18 percentage points), highlighting a sensitivity to temporal resolution. In contrast, EEGXF remains remarkably stable, with an accuracy drop of less than 2%. This reveals a key trade-off: S5 offers superior peak performance and speed, but EEGXF is preferable for applications with variable sampling rates.

Table 3. Zero-shot accuracy at different sampling rates.

Model	250Hz	128Hz	64Hz
S5	53.1%	37.5%	34.4%
EEGXF	40.9%	39.7%	40.7%

Figure 3 highlights the trade-off between speed and ro-

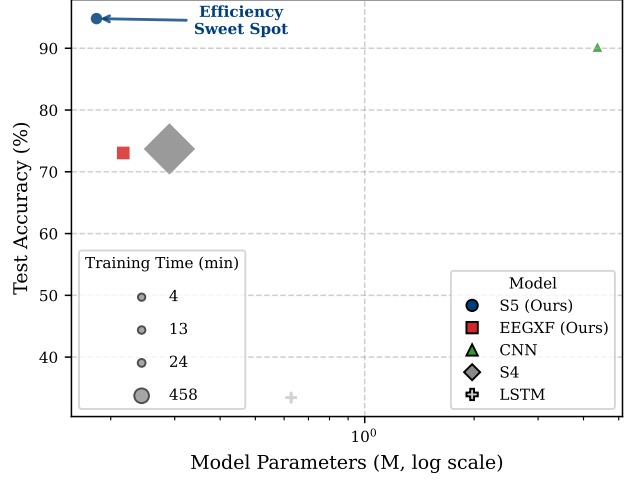


Fig. 2. Performance–efficiency trade-off at 64 s. Single-seed comparison of five architectures; accuracy vs. parameters (log-scale); marker size \propto training time (min). CNN is fastest (4.4 M parameters) while S5 (0.2 M parameters) attains state-of-the-art accuracy with $\sim 20\times$ fewer parameters than CNN; EEGXF is comparable in training time but less accurate.

bustness: S5 trains faster and achieves higher peak accuracy, but EEGXF is more stable under sampling frequency changes.

5.2. Leave-One-Subject-Out Generalization

To rigorously assess subject-independent generalization, we conducted a full leave-one-subject-out (LOSO) evaluation on 32 s segments. We ran 60 LOSO folds (multiple sessions per subject); significance tests used the 20 folds available for both models. The results (Table 4) confirm **S5’s architecture is superior for cross-subject generalization**, achieving a mean accuracy of 55.9%. While these scores are substantially lower than subject-mixed results and exhibit high variance (accuracies per fold ranged from 21% to 100%), they highlight the profound difficulty of cross-subject EEG decoding.

Table 4. Leave-One-Subject-Out (LOSO) performance on 32 s segments across 40 subjects. S5 demonstrates stronger cross-subject generalization.

Model	Mean Acc. (%)	Std. Dev.	Folds Run	Mean Time/Fold
S5	55.9	15.9	60 / 60	~41 min
EEGXF	48.4	12.1	20 / 60	~52 min

Statistical significance. Across the 20 matched LOSO folds, S5 outperformed EEGXF by 10.6 ± 15.1 pp in accuracy ($t_{19} = 3.13$, $p = 0.0055$) and 0.25 ± 0.16 in F1-score ($t_{19} = 7.05$, $p = 1.0 \times 10^{-6}$), with medium-to-large effect sizes. A McNemar test confirmed that S5 was significantly more likely to exceed 50% accuracy across folds ($\chi^2 = 12.0$,

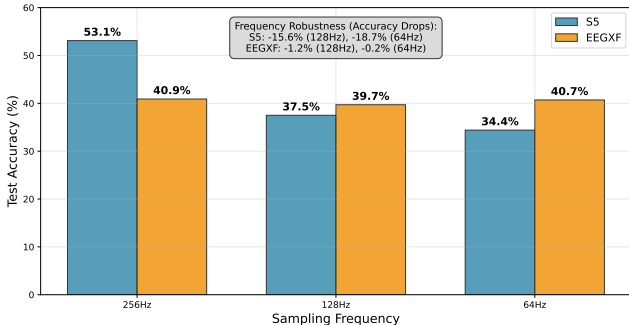


Fig. 3. Zero-shot generalization performance at different sampling frequencies. S5 shows a large drop in accuracy when tested on downsampled EEG, while EEGXF remains robust. This highlights a speed-accuracy-robustness trade-off across architectures.

$p = 4.9 \times 10^{-4}$). These findings reinforce that S5 generalizes better than EEGXF despite its overconfidence issues.

5.3. Zero-Shot Cross-Task Generalization

To test how models behave on unseen cognitive states, we evaluated our movie-trained models on three out-of-distribution (OOD) active tasks ($N = 245$). The results reveal a striking difference in generalization strategy, supported by calibration metrics on the in-distribution test set (Table 6).

S5 exhibited overconfident specialization. While it is exceptionally well-calibrated on in-distribution data, achieving the best NLL and Brier and near-best ECE (on par with CNN), it consistently misclassified all OOD tasks as ‘Movie 3’ with a high mean confidence of 60.0% (Table 5). Its failure to express uncertainty on novel inputs is a critical limitation.

In stark contrast, **EEGXF demonstrated a “conservative collapse.”** Although less calibrated on in-distribution data, it correctly identified the OOD tasks as unfamiliar by defaulting to its most neutral known class (‘Resting State’) with an appropriately low confidence of 26.0%. This behavior is not a failure but a sign of robust uncertainty quantification, a vital property for safe real-world deployment.

6. DISCUSSION AND CONCLUSION

Our systematic benchmark reveals a critical accuracy-efficiency-robustness trade-off in EEG decoding. In subject-mixed settings, both CNN and S5 architectures demonstrate powerful scaling with temporal context. However, S5 achieves this high performance with over 20x fewer parameters and greater training efficiency. Furthermore, in more challenging subject-independent tests (LOSO), S5’s superiority in learning generalizable features becomes even more evident.

However, this efficiency comes at the cost of robustness.

Table 5. Zero-shot cross-task generalization on unseen active tasks ($N=245$) and an in-distribution control task ($N=525$).

Model	Task Input	Dominant Prediction	Mean Confidence
<i>Out-of-Distribution (Active Tasks)</i>			
S5 (Specialized)	Symbol Search	Movie 3	60.0%
	Contrast Change	Movie 3	60.0%
	Spatial Memory	Movie 3	60.5%
EEGXF (Robust)	Symbol Search	Resting State	26.0%
	Contrast Change	Resting State	26.0%
	Spatial Memory	Resting State	26.0%
<i>In-Distribution Control</i>			
S5	Resting State	Resting State	> 95.0%
EEGXF	Resting State	Resting State	> 90.0%

Table 6. Calibration metrics (64 s, in-distribution). Lower is better.

Model	NLL \downarrow	Brier \downarrow	ECE (%) \downarrow
S5	0.056 \pm 0.008	0.006 \pm 0.002	1.09 \pm 0.12
EEGXF	0.999 \pm 0.023	0.077 \pm 0.005	13.41 \pm 1.68
CNN	0.079 \pm 0.014	0.007 \pm 0.002	0.96 \pm 0.20

Our novel cross-task generalization test demonstrates that S5 is prone to overconfident, incorrect predictions on unseen tasks. Conversely, EEGXF’s “conservative collapse” to a neutral, low-confidence state represents superior uncertainty handling. This trade-off forces a practical choice: S5 is ideal for speed in controlled settings, while EEGXF is preferable for robustness.

We acknowledge that this study relies on the HBN dataset to probe long-context scaling; future work should validate these architectural findings on standard benchmarks like Sleep-EDF. Additionally, while shorter segments used single seeds due to computational constraints, the multi-seed evaluation of key long-context results ensures the primary findings are robust.

7. REFERENCES

- [1] Seyed Yahya Shirazi, Alexandre Franco, Mauricio Scopel Hoffman, Nathalia Esper, Dung Truong, Arnaud Delorme, Michael Milham, and Scott Makeig, “The Healthy Brain Network EEG Datasets (HBN-EEG),” 2024.
- [2] Yannick Roy, Hubert Banville, Isabela Albuquerque, Alexandre Gramfort, Tiago H Falk, and Jocelyn Faubert, “Deep learning-based electroencephalography analysis: a systematic review,” *Journal of Neural Engineering*, vol. 16, no. 5, pp. 051001, 2019.
- [3] Robin Tibor Schirrmeister, Jost Tobias Springenberg, Lukas Dominique Josef Fiederer, Martin Glasstetter, Katharina Eggensperger, Michael Tangermann, Frank Hutter, Wolfram Burgard, and Tonio Ball, “Deep learning with convolutional neural networks for eeg decoding and visualization,” *Human brain mapping*, vol. 38, no. 11, pp. 5391–5420, 2017.
- [4] Ashish Vaswani, Noam Shazeer, Niki Parmar, Jakob Uszkoreit, Llion Jones, Aidan N Gomez, Łukasz Kaiser, and Illia Polosukhin, “Attention is all you need,” in *Advances in Neural Information Processing Systems (NeurIPS)*, I. Guyon, U. V. Luxburg, S. Bengio, H. Wallach, R. Fergus, S. Vishwanathan, and R. Garnett, Eds. 2017, vol. 30, pp. 5998–6008, Curran Associates, Inc.
- [5] Albert Gu, Karan Goel, and Christopher Ré, “Efficiently modeling long sequences with structured state spaces,” 2022.
- [6] Albert Gu and Tri Dao, “Mamba: Linear-Time Sequence Modeling with Selective State Spaces,” 2023.
- [7] Jiquan Wang, Sha Zhao, Zhiling Luo, Yangxuan Zhou, Shijian Li, and Gang Pan, “Eegmamba: An eeg foundation model with mamba,” *Neural Networks*, 2025.
- [8] Gourav Siddhad, Sayantan Dey, and Partha Pratim Roy, “Drowzee-g-mamba: Leveraging eeg and state space models for driver drowsiness detection,” in *International Conference on Pattern Recognition (ICPR)*. 2024, vol. 15327 of *Lecture Notes in Computer Science*, pp. 281–295, Springer.
- [9] Xuan-The Tran, Linh Le, and Chin-Teng Lin, “Eeg-ssm: Leveraging state-space model for dementia detection,” *arXiv preprint arXiv:2407.17801*, 2024.
- [10] Xinying Li, Shengjie Yan, Yonglin Wu, Chenyun Dai, and Yao Guo, “A novel state space model with dynamic graph neural network for eeg event detection,” *International Journal of Neural Systems*, vol. 35, no. 03, pp. 2550008, 2025.
- [11] Yonghao Song, Zhengyu Jia, and Mingsheng Li, “EEG-Conformer: A Hybrid Framework for Cross-Subject EEG-Based Emotion Recognition,” *IEEE Transactions on Affective Computing*, pp. 1–12, 2023.